Shapley value-based cost allocation for Battery Energy Storage Systems in Power Grids with a High Share of Renewables

Rebecca Bauer
Karlsruhe Institute of Technology
Karlsruhe, Germany
rebecca.bauer@kit.edu

Xinliang Dai
Karlsruhe Institute of Technology
Karlsruhe, Germany
xinliang.dai@kit.edu

Frederik Zahn
Karlsruhe Institute of Technology
Karlsruhe, Germany
frederik.zahn@kit.edu

Veit Hagenmeyer
Karlsruhe Institute of Technology
Karlsruhe, Germany
veit.hagenmeyer@kit.edu

Abstract

Battery energy storage systems (BESS), e.g., grid boosters, are becoming increasingly important for the stable, robust, and flexible operation of the transmission power grid. BESS can decrease costly re-dispatch measures by providing additional capacity in the grid. They can enhance congestion management through peak shifting and even reduce the need for expensive new transmission lines. For these benefits, a critical challenge is their efficient placement in the grid and their dimensioning. Our work adds to BESS placement evaluation by proposing a novel utility measure for the use of a storage unit. The proposed utility measure is based on the Shapley value from cooperative game theory. As a storage shows its benefit over time, the measure is evaluated on a horizon using multi-period AC optimal power flow. We test our approach on a radial five-node test grid and a modified IEEE case14 grid, including storage units and renewable energy sources that can be curtailed. The results show that the proposed method is able to evaluate the BESS' utility, including the provided reactive power compensation.

Keywords

Battery energy storage systems, flexibility, transmission grid, renewables, utility function

ACM Reference Format:
Rebecca Bauer, Xinliang Dai, Frederik Zahn, and Veit Hagenmeyer. 2025. Shapley value-based cost allocation for Battery Energy Storage Systems in Power Grids with a High Share of Renewables. In *The 16th ACM International Conference on Future and Sustainable Energy Systems (E-ENERGY '25), June 17–20, 2025, Rotterdam, Netherlands.* ACM, New York, NY, USA, 6 pages. https://doi.org/10.1145/3679240.3734664

E-ENERGY '25, Rotterdam, Netherlands

ACM ISBN 979-8-4007-1125-1/25/06
https://doi.org/10.1145/3679240.3734664

1 Introduction

The share of renewable energy sources (RES) in power grids has increased rapidly in recent years, bringing new challenges: volatility, high generation peaks, and a lack of grid inertia. To prevent congestions and blackouts and, hence, to ensure a stable operation, the transmission system operators (TSOs) need to perform increasingly many redispatch measures, which incur high costs.

To tackle these challenges, adding grid capacity to the grid by building new transmission lines is a potential long-term solution, however, expensive and slow. More flexibility and automated control are required. Battery Energy Storage Systems (BESS) can provide all of these, including a range of ancillary services [2, 9, 10], such as reactive power compensation [4]. BESS can alleviate transmission congestion [6] and enhance overall grid stability [12]. Their optimal placement in the grid, however, is a non-trivial task. The potential of BESS to reduce overall operation costs raises a critical question — *How much does each BESS unit contribute to lowering the respective costs?*

The present paper proposes a utility measure to quantify each BESS unit's contribution to the cost reduction in electricity grids. Due to nonlinear grid dynamics, we cannot simply apply the proportional method, i.e., their utility is proportional to power output. We choose the Shapley value from collaborative game theory [1], which gives a fair allocation. The Shapley value has been used in various fields such as social networks [11] and AI [16]. In the field of electricity grids, it has been mainly applied to distribution grids [15, 18] with a different focus, e.g., resource sharing [18]. In transmission grids, the Shapley value has been used to allocate transmission usage or network costs [14], e.g., grid-boosters, and, more recently, to share congestion management costs among system operators, both on a static AC-OPF [3] and on a multi-period DC-OPF [19]. However, none of these works include BESS in the OPF, or a multi-period OPF, and most papers use the approximate DC-OPF formulation.

The novelty of this approach, compared to previous work [3], is the extension of the Shapley value to a time horizon and its application to BESS. This approach provides a transparent and explainable way to assess the value of BESS in transmission grid operations. The main contributions of the present paper are:

- We extend the Shapley value to an OPF with multiple time periods.
- We apply the Shapley value to BESS as a utility measure.
- We demonstrate the utility value on the radial IEEE case5 and on the modified meshed IEEE case14.
- We show that the utility value reflects the BESS contribution to reactive power compensation.

The paper is organized as follows: Section 2 discusses the modeling of the grid, and the multi-period AC-OPF model including BESS. Section 3 recalls the Shapley value and defines its novel adaptation for BESS. Section 4 presents the simulation results, and Section 5 concludes the work and gives an outlook on future research.

2 Modelling

To assess a storage unit's utility for the grid, its operation must be evaluated over a time horizon $\mathcal{T} = \{1, \ldots, T\}$. The problem is solved on a grid $\mathcal{G} = (\mathcal{N}, \mathcal{L})$, with bus set $\mathcal{N} = \{1, \ldots, N_b\}$ and branch set $\mathcal{L} = \{1, \ldots, N_l\}$, with number of buses $N_b = |\mathcal{N}|$ and branches $N_l = |\mathcal{L}|$. The AC power flows are given by the active power P_i and reactive power Q_i for every load d_i and generator g_i at a bus $i \in \mathcal{N}$, and for the power flows f_{ij} on branch $l = (i, j) \in \mathcal{L}$, as well as by the voltage magnitude V_i and voltage angle θ_i.

2.1 Multi-Period OPF Formulation

To optimize storage schedules for active and reactive power, as well as curtailment costs, we solve a multi-period optimal power flow (MP-OPF) problem. Our formulation mostly follows [8, 13]. The MP-OPF is formulated as a nonlinear optimization problem, which we describe in the following.

The objective function Φ in (1) sums up all linear costs P for generation and curtailment of RES over all buses $\mathcal{N}$ and the time horizon $\mathcal{T}$, i.e.,

$$\Phi(P) = \sum_{t=1}^{T} \sum_{i=1}^{N_b} c_{G,i} \cdot P_{G,i}^t + c_{Curt,i} \cdot P_{Curt,i}^t + c_{S,i} \cdot P_{S,i}^t + c_i^0, \quad (1)$$

where $P_{G,i}^t, P_{Curt,i}^t$, and $P_{S,i}^t$ are the active power generation, curtailment, and storage injection at bus i, weighted with linear cost coefficients $c_{G,i}$, $c_{Curt,i}$, a constant cost coefficient c_i^0, and zero cost for storage use, i.e., $c_{S,i} = 0$.

The power flow equations in the MP-OPF problems can be summarized as the active and reactive power nodal balances

$$\sum_{j=1}^{N_b} V_i^t V_j^t \left(G_{ij} \cos\theta_{ij}^t + B_{ij} \sin\theta_{ij}^t \right) = P_{G,i}^t - P_{D,i}^t + P_{S,i}^t + P_{Curt,i}^t, \quad (2a)$$

$$\sum_{j=1}^{N_b} V_i^t V_j^t \left(G_{ij} \sin\theta_{ij}^t - B_{ij} \cos\theta_{ij}^t \right) = Q_{G,i}^t - Q_{D,i}^t + Q_{S,i}^t + Q_{Curt,i}^t, \quad (2b)$$

$\forall i \in \mathcal{N}$, $\forall t \in \mathcal{T}$, where $P_{D,i}^t, Q_{D,i}^t$ are the active and reactive power of the laod, V_i^t denotes the voltage magnitude at bus $i \in \mathcal{N}$ and $\theta_{ij}^t = \theta_i - \theta_j$ denotes the voltage angle difference between bus i and bus j along the branch $(i, j) \in \mathcal{L}$ at time t. Variables B_{ij}, G_{ij} represent the real and imaginary parts of the complex admittance matrix Y, respectively. Moreover, $P_{S,i}^t$, $P_{Curt,i}^t$, and $P_{D,i}^t$ denote the active power injections at bus i at time t from storage, renewable generation curtailment, and RES, respectively. The corresponding power injections are set to zero if no storage, renewable generation, or RES is connected to bus $i \in \mathcal{N}$.

These variables are subject to their physical constraints:

$$\underline{P}_{G,i} \leq P_{G,i}^t \leq \overline{P}_{G,i}, \quad \underline{Q}_{G,i} \leq Q_{G,i}^t \leq \overline{Q}_{G,i}, \quad (3a)$$

$$\underline{V}_i \leq V_i^t \leq \overline{V}_i, \quad \underline{\theta}_{ij} \leq \theta_{ij}^t \leq \overline{\theta}_{ij}, \quad (3b)$$

$$-\overline{P}_{Curt,i}^t \leq P_{Curt,i}^t \leq 0, \quad (3c)$$

$$|f_{ij}^t| \leq \overline{F}_{ij}, \quad (3d)$$

$\forall i \in \mathcal{N}$, $\forall t \in \mathcal{T}, \forall (i,j) \in \mathcal{L}$, with the definition of the branch flow magnitude $|f_{ij}^t|$ at time t:

$$|f_{ij}^t| = \sqrt{(Q_{ij}^t)^2 + (P_{ij}^t)^2},$$

where (3a) give the capacity limits of active and reactive power generation, (3b) the limits for voltage magnitude and voltage angle, (3c) the maximum curtailment bounded by RES generation and (3d) the thermal branch limits.

The BESS model consists of the physical limits:

$$P_{S,i}^t = P_{S,i}^{t,CH} - P_{S,i}^{t,DC}, \quad P_{S,i}^{t,CH} \cdot P_{S,i}^{t,DC} = 0 \quad (4a)$$

$$0 \leq P_{S,i}^{t,CH} \leq \overline{P}_{S,i}, \quad 0 \leq P_{S,i}^{t,DC} \leq \overline{P}_{S,i}, \quad (4b)$$

$$\underline{Q}_{S,i} \leq Q_{S,i}^t \leq \overline{Q}_{S,i}, \quad (4c)$$

$$0 \leq SoC_i^t \leq \overline{SoC}, \quad (4d)$$

as well as the charging and discharging relationship:

$$SoC_i^t = SoC_i^{t-1} \eta_{S,i}^{SDC} + \Delta t (\eta_{S,i}^{CH} P_{S,i}^{t,CH} - \frac{1}{\eta_{S,i}^{DC}} P_{S,i}^{t,DC}), \quad (4e)$$

$\forall i \in \mathcal{N}$, $\forall t \in \mathcal{T}$. The corresponding variables are set to zero if no storage is connected to bus $i \in \mathcal{N}$. In the present paper, the charging and discharging are modeled by the two variables $P_{S,i}^{t,CH}, P_{S,i}^{t,DC}$ adding to the storage power $P_{S,i}^t$ with the complementary constraint (4a) to prevent simultaneous charging and discharging. The technical limits for the maximal active and reactive power, charging and discharging, as well as the maximum capacity as the state of charge, are given by (4b)-(4d). The coupling constraint (4e) gives the state of charge SoC_i^t at time t, including the charging, discharging, and self-discharging efficiencies $\eta_{S,i}^{CH}, \eta_{S,i}^{DC}, \eta_{S,i}^{SDC} \in (0, 1]$.

Combining equations (1)-(4) we obtain the AC MP-OPF.

3 Utility measure for BESS

With the storage schedules and generation costs from the MP-OPF, we construct a utility measure that also considers the time horizon $\mathcal{T}$. The utility measure is based on the Shapley value

[1], which is based on a cost function, e.g., an OPF, and defined in Section 3.1. To apply it to a MP-OPF, we define the Shapley value for BESS on multiple time periods $t = 1, \dots, T$ in Section 3.2.

3.1 The Shapley Value

The Shapley value is a cost allocation method that fairly distributes costs or profits among multiple actors. It is the only allocation key that fulfills the fairness axioms [1]. In this context, the profit represents the cost reduction through BESS. Let $(\mathcal{P}, \Phi)$ represent a game, where $\mathcal{P}$ is a set of players, i.e., BESS units, and Φ is the objective function of the MP-OPF that assigns costs to different coalitions (subsets of players), i.e., $\Phi(\Omega)$, where Ω refers to a group of players in collaboration, i.e., simultaneously operating BESS units. In this paper, we use the Shapley value to distribute the costs of the grand coalition $\Omega = \mathcal{P}$, i.e., when all storage units are in use, to each player $p = s_i \subset \mathcal{S} = \mathcal{P}$ with a contribution of Ψ.

The Shapley value is defined as the average marginal contributions of p to all coalitions $\Omega \subset \mathcal{P}$:

$$\Psi_p(\Phi) = \sum_{\Omega \in \mathcal{P} \setminus \{p\}} \frac{|\Omega|! \left(|\mathcal{P}| - |\Omega| - 1\right)!}{|\mathcal{P}|!} \left\{\Phi\left(\Omega \cup p\right) - \Phi\left(\Omega\right)\right\}, \tag{5}$$

where $\Phi(\Omega \cup p) - \Phi(\Omega)$ is the marginal contribution of the player p, weighted with the chance of occurrence of the coalition Ω. This leads to a computational complexity of $O(2^n)$ for $n = |\mathcal{P}|$ players, making the Shapley value challenging for large $n \gtrsim 10$. In transmission grids, where only a few but large BESS are installed, our approach still allows for evaluating selected strategic BESS locations. If needed, several approximations exist for the Shapley [5, 7, 17].

In the following, we adapt this notation to BESS.

3.2 Adapting the Shapley Value to BESS

In our setting, the utility of a BESS unit is defined by the individual contribution to the reduction of costs that the unit achieves. As in the previous section, we set the storage units $\mathcal{S}$ as the set of players $\mathcal{P}$, and the MP-OPF (1)-(4) as the cost function Φ. A coalition $\Omega \subset \mathcal{S}$ represents the simultaneous activation of a subset of BESS.

To apply the Shapley value of a storage unit $s_i \in \mathcal{S}$ to a MP-OPF, we can take the cost value for each time step Φ^t, then sum the values over $\mathcal{T}$, average them with T to avoid accumulation, and multiply by -1 to turn the negative cost reduction into a positive utility value:

$$\Psi_p^{BESS}(\Phi) = -\frac{1}{T} \sum_t \Psi_p^t(\Phi^t). \tag{6}$$

This value quantifies the contribution of a BESS unit to the overall cost reduction.

The notation can be simplified due to the linearity of the cost function, i.e., the sum of the costs of each time step $\sum \Phi^t$ simply yields the overall cost Φ of the MP-OPF, and the additivity axiom of the Shapley value [1] . Hence, equation (6) reduces to:

$$\Psi_{s_i}^{BESS}(\Phi) = -\frac{1}{T} \cdot \Psi_{s_i}(\Phi) \tag{7}$$

The Shapley algorithm works as follows: Given a set of storage units $\mathcal{S} = \mathcal{P}$ (players), we compute the MP-OPF with the respective subset of storage units for all coalitions $\Omega \subset \mathcal{P}$ and save the costs (generation and curtailment). With these total costs, we can compute the Shapley value Ψ_p for each player as the average sum of weighted marginal contributions to all coalitions.

4 Simulation Results

We demonstrate our approach on a radial five-node test grid and a modified meshed IEEE case14 standard grid with a time horizon of 12 hours. Our computations for the MP-OPF are implemented in the JULIA-language, using the packages POWERMODELS.JL and JUMP, combined with the solver IPOPT.

4.1 Baseline

As a baseline to evaluate the performance of a storage s_i, we take the active power injections summed over the horizon $\mathcal{T}$:

$$B_i = \sum_{t \in \mathcal{T}} P_{S,i}^{t,DC}, \tag{8}$$

$i \in \mathcal{N}$. Note that this is equal to using $P_{S,i}^{t,CH}$ as the state of charge must be the same in the beginning as in the end.

4.2 Load & RES Data Generation

For load and RES generation, we use synthetic data. The time series for load and RES are constructed with sine curves to imitate periodic load and generation patterns. The load function $\mathrm{d_i}^{laod}$ is given by

$$f_{load,i} = |d_i^{load} \cdot \frac{1}{2} \cdot \gamma^{load} \cdot (\sin(\frac{t\pi}{T}))|, \tag{9}$$

with initial load d_i^{load}, scaling factor $\gamma^{load} \in \mathbb{R}$, and $f_{load,i} \geq 0$. Its evaluation on the horizon $\mathcal{T}$ yields the load vector $\mathrm{d_i} = f_{load,i}|_{\mathcal{T}} \in \mathbb{R}^T$. The function $f_{RES,i}$ for the RES (negative load) is given by

$$f_{RES,i} = -|d_i^{RES} \cdot \frac{1}{2} \cdot \gamma^{RES} \cdot \left(\sin(\frac{4t\pi}{T} + 0.7) + \sin(\frac{3t\pi}{T})\right)|, \tag{10}$$

with initial generation d_i^{RES}, scaling factor $\gamma^{RES} \in \mathbb{R}$ and $f_{RES,i} \leq 0$ (negative load equals generation). Its evaluation on the horizon $\mathcal{T}$ yields the RES generation vector $\mathrm{d_i}^{RES}|_{\mathcal{T}} \in \mathbb{R}^T$.

4.3 Radial Five-Node Test Grid

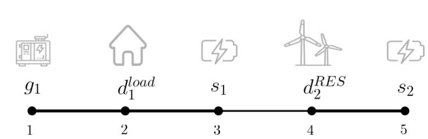

Figure 1: Grid topology and bus types for case5.

The five-node test grid is shown in Figure 1. The grid consists of five nodes and four branches, with one generator located at one end, followed by a load, a storage unit, renewable generation, and a second storage unit at the other end. The

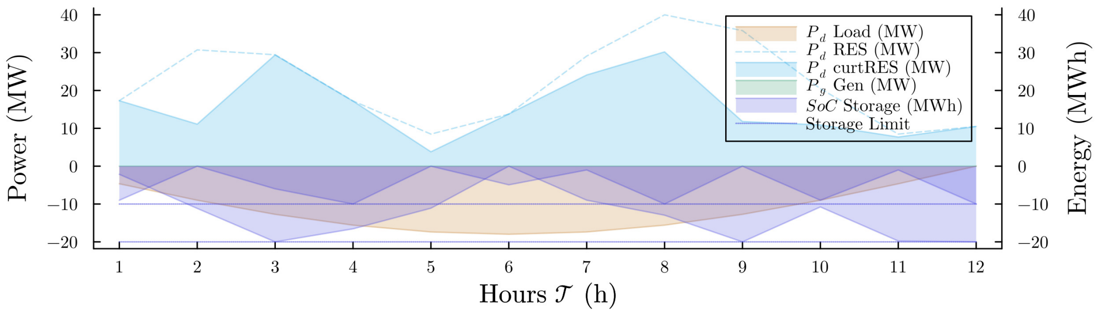

Figure 2: OPF results of case5 for the grand coalition $\Omega = \{3, 5\}$.

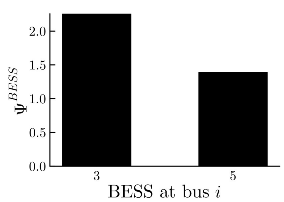

(a) Shapley values.

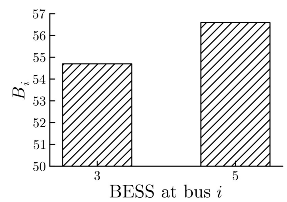

(b) Baseline.

Figure 3: Shapley values and the summed active power injections for the three storage units s_3 and s_5 of case5.

branch capacity is 100, and reduced to 40 MWA at branch (2, 3) to create a congestion. The load is 40 MW/20 MWh, RES is 30 MW/10 MWh, the generation cost is €40, and the curtailment cost is €60 per MWh. Storage limits for units s_3 and s_5 are 20 MWh and 10 MWh, respectively, with reactive power limits of [-50, 70] MVA and efficiencies of 0.9.

The OPF results of case5 of the grand coalition $\Omega = \{3, 5\}$ with both storage units at node $i = 3$ and node $i = 5$ active are depicted in Figure 2. We can see that the RES generation covers the entire load with some curtailment so that no conventional generation is required. Both storage units are charged and discharged repeatedly, while s_3 has twice as much capacity and stores more energy. Without storage (empty coalition $\Omega = \{\}$), conventional generation ramps up.

Table 1: Costs of coalitions for case5.

Coalition Ω	$\{\}$	$\{3\}$	$\{5\}$	$\{3, 5\}$
Cost Φ (€)	87.8	55.8	66.2	44.0

Looking at the costs in Table 1, we can see that both storage units together give a reduction in costs of 49.8%, while storage unit 3 reduces the MP-OPF costs a little more. Hence, storage s_3 seems more beneficial.

The Shapley values in Figure 3a confirm this expectation. We can see that the storage unit s_3 has a higher utility value of 2.26 than s_5 with a value of 1.39. This is in accordance with the MP-OPF results and with the fact that storage s_3 lies in the middle of the grid and is of larger size. However, checking the sum of the total active power injections in Figure 3b— on which the objective function builds —we see that the injections of storage s_5 with 56.6 MW are higher than those of s_3 with 54.8 MW. Hence, storage s_3 must provide some additional contribution.

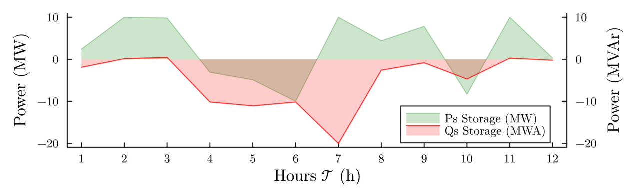

(a) Storage unit s_3.

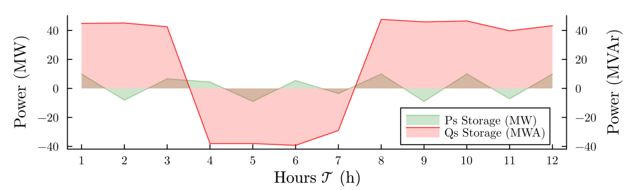

(b) Storage unit s_5.

Figure 4: Active (green) and reactive power input (red) of the BESS units of case5.

A closer look at the storage variables explains this observation. Figure 4 shows the active power and reactive power of both storage units. We can see that the active power goes hand in hand with the state of charge in Figure 2, as it is its derivative. The reactive power, however, provides additional information. We can see that for storage unit s_3 it somewhat follows the state of charge in between the interval [-20,0] MVA. For storage unit s_5, however, it dis-/charges a lot more reactive power in the interval [-40,45] MVA, which is reactive power compensation. Hence, the contribution reactive power is captured by the Shapley value as it influences power generation through line losses and voltage angles.

4.4 Modified IEEE case14

A more complex example is the IEEE case14, which has more nodes and is a meshed grid; see Figure 6. The loads and RES are

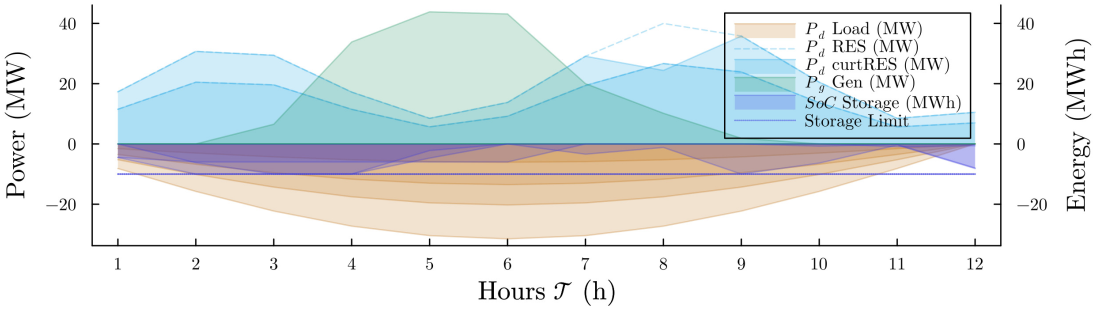

Figure 5: OPF results of case5 for the grand coalition $\Omega = \{3, 5\}$.

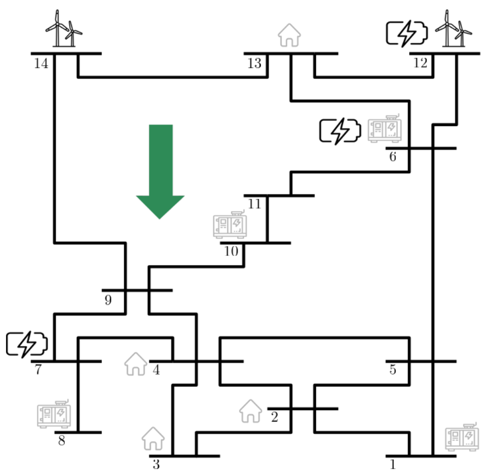

Figure 6: Scenario for IEEE case14.

Table 2: Costs of coalitions for case14.

Ω	{}	{6}	{7}	{12}	{6, 7}	{6, 12}	{7, 12}	{6, 7, 12}
Φ (€)	81.8	68.0	69.4	63.8	63.2	51.2	51.7	48.9

concentrated in order to make the power flows more understandable and to imitate real-world situations. The most important parameters different to case5 are: The loads d_2, d_3, d_4, d_{13} are set to 45 MW/14 MWA, 30 MW/10 MWA, 70 MW/25 MWA, and 13 MW/6 MWA, respectively, and RES $d_{12}^{RES}, d_{14}^{RES}$ to 30 MW/10 MWA and 20 MW/7 MWA, respectively. Generation costs are €20, €30, €35, €40, and €50 for plants $g_{10}, g_1, g_2, g_8, g_6$, respectively. Branches (4, 9), (5, 6), (6, 12), (7, 8), (12, 13) have a reduced capacity of 30 MWA, and the storage capacities are all 10 MWh.

The OPF results of case14 are given in Figure 5. We can see that the RES generation is insufficient for the load, as conventional generation fills in. Several storage units are charged, discharged, and charged again during the second peak. Removing the BESS results in a significantly higher conventional generation, while some curtailment still occurs during peak periods, which is likely due to the restricted line capacity from north to south.

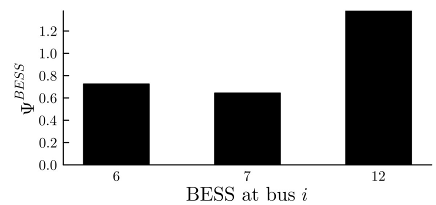

Figure 7: Shapley values for three storage units s_6, s_7 and s_{12} for case14.

Looking at the costs in Table 2, it seems that storage s_{12} contributes most to cost reduction on its own, followed by s_6 and s_7 last. The overall cost reduction from 81.8€ to 48.9€ is approximately 40%. This is fairly similar to the case5 scenario, presumably due to the chosen cost values.

The Shapley values in Figure 7 confirm this observation, as unit s_{12} has the largest contribution of 1.38, followed by storage units s_6 and s_7 with 0.72 and 0.64. In this example, the Shapley values roughly correspond to the summed active power up to size. Still, we need to check the reactive power.

In Figure 8 we see that units s_6 and s_7 significantly contribute to reactive power compensation up to 70 MVAr. Despite s_{12} having lower values in the range of [-5,10], its Shapley value is greater. The probable explanation is that active power contributes more to cost reduction than reactive power.

4.5 Insights

From these two use cases, we can conclude two main results.

1. The contribution of one storage unit cannot be directly derived from the active power injections resulting from the MP-OPF, for neither the radial nor the meshed grid.
2. The Shapley value captures the effect of reactive power compensation from BESS, even though the costs of the MP-OPF only include active power generation.

From the preceding points, it becomes clear that the Shapley value can contribute to increased transparency regarding the utility of BESS units for the power grid.

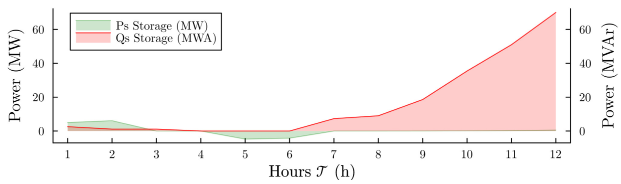

(a) Storage unit s_6.

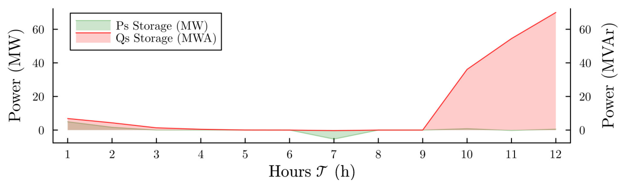

(b) Storage unit s_7.

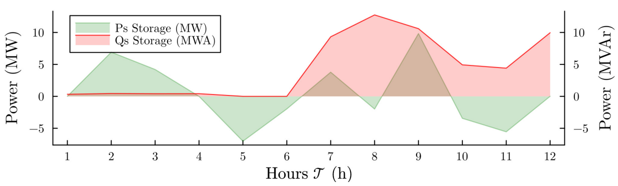

(c) Storage unit s_{12}.

Figure 8: Active (green) and reactive power input (red) of the BESS units of case14.

5 Conclusion

The increasingly complex and growing power systems call for greater transparency and explainability of their inner workings and increased control. This paper introduces a new utility measure for Battery Energy Storage Systems (BESS) using the Shapley value based on multi-period optimal power flow. It provides greater transparency regarding the functionality of a BESS unit in the power grid. This can help TSOs decide where to place storage units and how to develop pricing incentives for BESS. The paper presents a proof-of-concept on two test grids: a radial five-node test grid for simplicity and a modified IEEE 14-case grid. Results show that comparably large BESS units can significantly reduce costs and contribute to reactive power compensation.

In future work, we plan to analyze the utility measure further in terms of robustness and sensitivity based on variations in several parameters, such as storage size, location, or the amount of renewable energy. Also, exploring the optimal horizon length required to achieve a stable Shapley value may be worthwhile. Furthermore, we plan to explore further how the Shapley value captures reactive power compensation and how it can be used for optimal placement analysis of BESS in the grid, especially regarding scalability. And lastly, the question arises whether we can apply the Shapley value to other MP-OPF outputs, such as solely reactive power or curtailment, to enhance transparency in the power grid further.

References

[1] Encarnación Algaba, Vito Fragnelli, and Joaquín Sánchez-Soriano. 2020. Handbook of the Shapley Value. (2020), 607.

[2] Ayesha, Muhammad Numan, Musaed Alhussein, Muhammad Faisal Baig, and Khursheed Aurangzeb. 2024. Enhancing grid flexibility with coordinated battery storage and smart transmission technologies. *Journal of Energy Storage* 100 (Oct. 2024), 113607. doi:10.1016/j.est.2024.113607

[3] Rebecca Bauer, Xinliang Dai, and Veit Hagenmeyer. 2024. Industrial Application of the Shapley value-based Redispatch Cost Allocation to Large-Scale Power Grids requires AC Optimal Power Flow. doi:10.48550/arXiv.2405.06439

[4] Nate Blair, Chad Augustine, Wesley Cole, Paul Denholm, Will Frazier, Madeline Geocaris, Jennie Jorgenson, Kevin McCabe, Kara Podkaminer, Ashreeta Prasanna, and Ben Sigrin. 2022. *Storage Futures Study: Key Learnings for the Coming Decades.* Technical Report. doi:10.2172/1863547

[5] Kevin Corder and Keith Decker. 2019. Shapley Value Approximation with Divisive Clustering. In *2019 18th IEEE International Conference On Machine Learning And Applications (ICMLA).* 234–239. doi:10.1109/ICMLA.2019.00044

[6] Ehsan Dehnavi, Farrokh Aminifar, and Saeed Afsharnia. 2019. Congestion management through distributed generations and energy storage systems. *International Transactions on Electrical Energy Systems* 29, 6 (2019), e12018. doi:10.1002/2050-7038.12018

[7] Shaheen S. Fatima, Michael Wooldridge, and Nicholas R. Jennings. 2008. A linear approximation method for the Shapley value. *Artificial Intelligence* 172, 14 (Sept. 2008), 1673–1699. doi:10.1016/j.artint.2008.05.003

[8] Georg Gutermuth and Marco Giuntoli. 2020. Network operator owned storages as an option for congestion management. In *2020 IEEE PES Innovative Smart Grid Technologies Europe (ISGT-Europe).* 1074–1078. doi:10.1109/ISGT-Europe47291.2020.9248825

[9] Yu Hu, Miguel Armada, and María Jesús Sánchez. 2022. Potential utilization of battery energy storage systems (BESS) in the major European electricity markets. *Applied Energy* 322 (Sept. 2022), 119512. doi:10.1016/j.apenergy.2022.119512

[10] Martin Lindner, Jan Peper, Nils Offermann, Charlotte Biele, Milijana Teodosic, Oliver Pohl, Julian Menne, and Ulf Häger. 2023. Operation strategies of battery energy storage systems for preventive and curative congestion management in transmission grids. *IET Generation, Transmission & Distribution* 17, 3 (2023), 589–603. doi:10.1049/gtd2.12739

[11] Ramasuri Narayanam and Yadati Narahari. 2011. A Shapley Value-Based Approach to Discover Influential Nodes in Social Networks. *IEEE Transactions on Automation Science and Engineering* 8, 1 (Jan. 2011), 130–147. doi:10.1109/TASE.2010.2052042

[12] Hung Cuong Nguyen, Quoc Tuan Tran, and Yvon Besanger. 2024. Effectiveness of BESS in Improving Frequency Stability of an Island Grid. *IEEE Transactions on Industry Applications* 60, 6 (Nov. 2024), 8203–8212. doi:10.1109/TIA.2024.3443241

[13] Nhi T. A. Nguyen, Duong D. Le, Cristian Bovo, and Alberto Berizzi. 2015. Optimal Power Flow with energy storage systems: Single-period model vs. multi-period model. In *2015 IEEE Eindhoven PowerTech.* 1–6. doi:10.1109/PTC.2015.7232438

[14] Pawan Rathore, Ganga Agnihotri, Baseem Khan, and Garima Naidu. 2014. Transmission Usage and Cost Allocation Using Shapley Value and Tracing Method: A Comparison. *Electrical and Electronics Engineering: An International Journal* 3, 3 (Aug. 2014), 11–29. doi:10.14810/elelij.2014.3302

[15] Satish Sharma and A. R. Abhyankar. 2017. Loss allocation of radial distribution system using Shapley value: A sequential approach. *International Journal of Electrical Power & Energy Systems* 88 (June 2017), 33–41. doi:10.1016/j.ijepes.2016.11.015

[16] Maurizio Titz, Sebastian Pütz, and Dirk Witthaut. 2024. Identifying drivers and mitigators for congestion and redispatch in the German electric power system with explainable AI. *Applied Energy* 356 (Feb. 2024), 122351. doi:10.1016/j.apenergy.2023.122351

[17] Tjeerd van Campen, Herbert Hamers, Bart Husslage, and Roy Lindelauf. 2017. A new approximation method for the Shapley value applied to the WTC 9/11 terrorist attack. *Social Network Analysis and Mining* 8, 1 (Dec. 2017), 3. doi:10.1007/s13278-017-0480-z

[18] Ivo A. M. Varenhorst, Johann Hurink, and Marco E. T. Gerards. 2024. Quantifying Device Flexibility With Shapley Values in Demand Side Management. doi:10.1145/3632775.3661950

[19] Simon Voswinkel. 2023. Simplifying the Computation of Shapley Values for Allocating Congestion Costs in Large Power Grid Models. *SSRN Electronic Journal* (2023). doi:10.2139/ssrn.4449794